



Contents lists available at ScienceDirect

## Journal of Molecular Liquids

journal homepage: [www.elsevier.com/locate/molliq](http://www.elsevier.com/locate/molliq)

# Synthesis of 1,3-thiazolidin-4-one using ionic liquid immobilized onto Fe<sub>3</sub>O<sub>4</sub>/SiO<sub>2</sub>/Salen/Mn

Q2 Q1 Seyed Mohsen Sadeghzadeh <sup>a,b,\*</sup>, Maryam Malekzadeh <sup>b</sup>

<sup>a</sup> Department of Chemistry, College of Sciences, Birjand University, P.O. Box 97175-615, Birjand, Iran

<sup>b</sup> Department of Chemistry, Payame Noor University, P.O. Box 19395-4697, Tabas, Iran

## ARTICLE INFO

## Article history:

Received 26 September 2014

Received in revised form 31 October 2014

Accepted 9 December 2014

Available online xxxx

## Keywords:

Multi-component cyclization

Magnetic nanoparticles (MNPs)

Salen

Green chemistry

Ionic liquid

1,3-Thiazolidin-4-one

## ABSTRACT

An efficient and general method has been developed for synthesis of 1,3-thiazolidin-4-ones using magnetite nanoparticles immobilized Salen–Mn–ionic liquids as an efficient and recyclable catalyst. The inorganic, magnetic, solid base catalyst was characterized via N<sub>2</sub> sorption, TEM, VSM, TGA, XRD, FTIR, and UV–vis. Nanocatalyst can be easily recovered by a magnetic field and reused for subsequent reactions for at least 6 times with less deterioration in catalytic activity.

© 2014 Published by Elsevier B.V.

## 1. Introduction

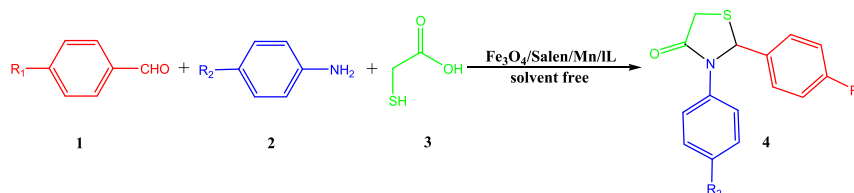
The thiazolidin-4-one ring system is a core structure found in various synthetic pharmaceutical compounds, displaying a broad spectrum of biological activities [1–6]. Consequently, several synthetic methods have been developed for the synthesis of 4-thiazolidinones. The main synthetic routes to thiazolidin-4-ones involve cyclocondensation of azomethines (Schiff's base) with mercaptoacetic acid [7]. There are also reports using chemical agents, such as N-methylpyridinium tosylate [8] as desiccant, to assist the formation of thiazolidinone derivatives. The use of [BmIm] OH [9], Hunig's base [10], and Baker's yeast [11] has also been reported to expedite the cyclo-condensation of the azomethines and thioglycolic acid.

Ionic liquids (ILs) have emerged as promising homogeneous catalysts [12] because of their unique physicochemical properties including negligible vapor pressure, wide liquid range, high ionic conductivity and excellent solubility [13]. Although ILs possess some advantages but their practical applications have been restricted by some difficulties in its recovery which lead to economical and environmental problems. On the other hand, their high viscosity not only limits their mass transfer during catalytic reactions but also makes their handling difficult. Moreover,

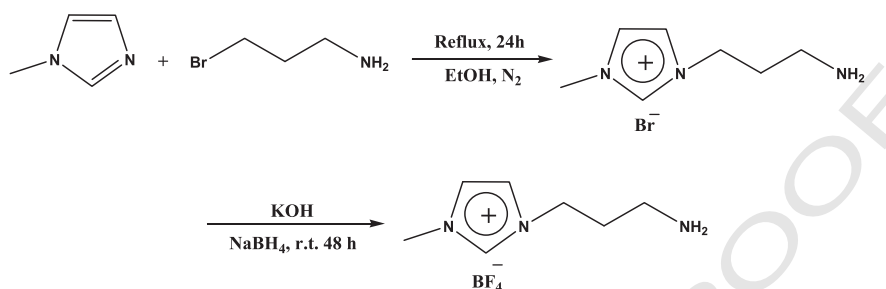
the use of relatively large amounts of ILs is costly and may cause toxicological concerns. These problems can be overcome by immobilization of ILs onto solid supports to obtain heterogeneous catalysts [14–16]. Thus, efforts have been made to immobilize them on diverse soluble and insoluble supports, such as inorganic solids [17–21], polymers [22,23], and nanoparticles [24–35]. Nowadays, magnetite nanoparticles, especially Fe<sub>3</sub>O<sub>4</sub> nanoparticles have attracted increasing interest because of their unique physical properties including the high surface area, superparamagnetism, low toxicity and their potential applications in various fields. The Fe<sub>3</sub>O<sub>4</sub> nanoparticles are easily prepared and surface functionalized and they can be recycled from the solution by external magnetic field. Hence, the catalyst supported on Fe<sub>3</sub>O<sub>4</sub> nanoparticles can be easily separated from the reaction system and reused. In addition, the reported coupling reactions were mostly carried out in organic solvents, to begin with environmental benign, the development of highly efficient heterogeneous catalysts to facilitate coupling reaction in benign medium is highly desirable.

In this work, our interest in this area led us to explore the Salen/Mn/ionic liquid (IL) immobilized onto the surface of magnetic nanoparticles, which can be sufficiently applied even for the synthesis 1,3-thiazolidin-4-one and then can be easily separated from the reaction mixture to reuse. Herein, we wish to describe the synthesis of reusable magnetite nanoparticles supported Salen/Mn/IL and its catalytic activity in the multicomponent reaction (Scheme 1).

\* Corresponding author at: Department of Chemistry, College of Sciences, Birjand University, P.O. Box 97175-615, Birjand, Iran.



**Scheme 1.** Synthesis of 1,3-thiazolidin-4-one in the presence of  $\text{Fe}_3\text{O}_4/\text{SiO}_2/\text{Salen}/\text{Mn}/\text{IL}$  MNPs.



**Scheme 2.** Synthesis of the ionic liquid (IL) containing primary amine.

## 2. Experimental

### 2.1. Materials and methods

Chemical materials were purchased from Fluka and Merck in high purity. Melting points were determined in open capillaries using an Electrothermal 9100 apparatus are uncorrected. FTIR spectra were recorded on a VERTEX 70 spectrometer (Bruker) in the transmission mode in spectroscopic grade KBr pellets for all the powders. Morphology was analyzed using high-resolution transmission electron microscopy (HRTEM) on a JEOL transmission electron microscope operating at 200 kV. The content of phosphorous in the catalyst was determined by OPTIMA 7300DV inductively coupled plasma (ICP) analyzer. Powder X-ray diffraction data was obtained using Bruker D8 Advance model with Cu K $\alpha$  radiation. The thermogravimetric analysis (TGA) was carried out on a NETZSCH STA449F3 at a heating rate of 10  $^{\circ}\text{C min}^{-1}$  under nitrogen. The magnetic measurement was carried out in a vibrating sample magnetometer (VSM) (4 in., Daghigh Meghnatis Kashan Co.,

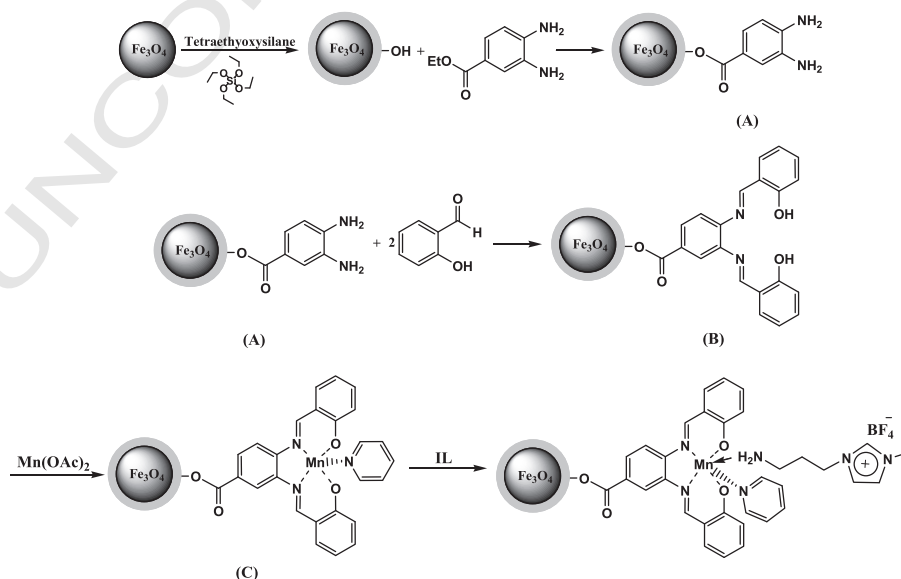
Kashan, Iran) at room temperature. NMR spectra were recorded in  $\text{CDCl}_3$  on a Bruker Avance DRX-400 MHz instrument spectrometer using TMS as internal standard. The purity determination of the products and reaction monitoring was accomplished by TLC on silica gel polygram SILG/UV 254 plates.

### 2.2. General procedure for the ionic liquid

The IL was prepared as described previously [36], which was outlined in Scheme 2.

### 2.3. General procedure for the preparation of $\text{Fe}_3\text{O}_4/\text{SiO}_2/\text{Salen}/\text{Mn}$ nanoparticles

$\text{Fe}_3\text{O}_4/\text{SiO}_2/\text{Salen}/\text{Mn}$  nanoparticles were prepared by a simple method in our previous work [37].



**Scheme 3.** Schematic illustration of the synthesis for  $\text{Fe}_3\text{O}_4/\text{SiO}_2/\text{Salen}/\text{Mn}/\text{IL}$  nanoparticles.

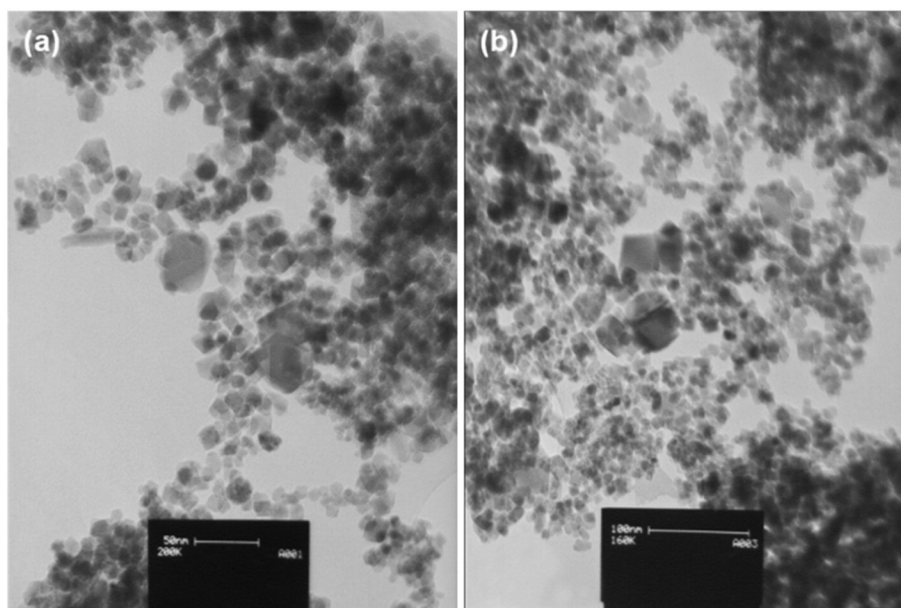


**Fig. 1.** TEM images of (a)  $\text{Fe}_3\text{O}_4/\text{SiO}_2/\text{Salen}/\text{Mn}/\text{IL}$  MNPs, and (b)  $\text{Fe}_3\text{O}_4/\text{SiO}_2/\text{Salen}/\text{Mn}/\text{IL}$  MNPs after six reuses.

#### 2.4. General procedure for the preparation of $\text{Fe}_3\text{O}_4/\text{SiO}_2/\text{Salen}/\text{Mn}/\text{IL}$ nanoparticles

IL (1 mmol) was dispersed in dry ethanol (20 ml) and  $\text{Fe}_3\text{O}_4/\text{SiO}_2/\text{Salen}/\text{Mn}$  (0.1 g) MNPs were added. Then the mixture was heated to  $60^\circ\text{C}$  for 12 h under nitrogen atmosphere. The resulting solid was separated by an external magnet and washed 3 times with  $\text{CH}_2\text{Cl}_2$ , ethanol

and  $\text{H}_2\text{O}$ . After drying at room temperature in vacuum,  $\text{Fe}_3\text{O}_4/\text{SiO}_2/\text{Salen}/\text{Mn}/\text{IL}$  MNPs were obtained as reddish-brown powder.

#### 2.5. General procedures for preparation of 1,3-thiazolidin-4-ones

A mixture of aldehyde (1 mmol), amine (1 mmol), thioglycolic acid (1 mmol), and  $\text{Fe}_3\text{O}_4/\text{SiO}_2/\text{Salen}/\text{Mn}/\text{IL}$  MNPs (0.0008 g) was stirred at room temperature under solvent-free conditions. Upon completion, the progress of the reaction was monitored by TLC when the reaction was completed, EtOH was added to the reaction mixture and the  $\text{Fe}_3\text{O}_4/\text{SiO}_2/\text{Salen}/\text{Mn}/\text{IL}$  MNPs was separated by external magnet. Then the solvent was removed from solution under reduced pressure and the resulting product purified by recrystallization using *n*-hexane/ethyl acetate.

#### 2.6. Selected spectral data of the products 2-(2-nitrophenyl)-3-p-tolylthiazolidin-4-one (4c)

IR (KBr):  $\nu = 3036, 2930, 1723, 1548, 1529$ , and  $1352\text{ cm}^{-1}$ ;  $^1\text{H}$  NMR (400 MHz,  $\text{DMSO}-d_6$ ):  $\delta = 8.01$  (d,  $J = 8.1\text{ Hz}$ , 1H), 7.70–7.73 (m, 2H), 7.47–7.52 (m, 1H), 7.36 (d,  $J = 8.3\text{ Hz}$ , 2H), 7.13 (d,  $J =$

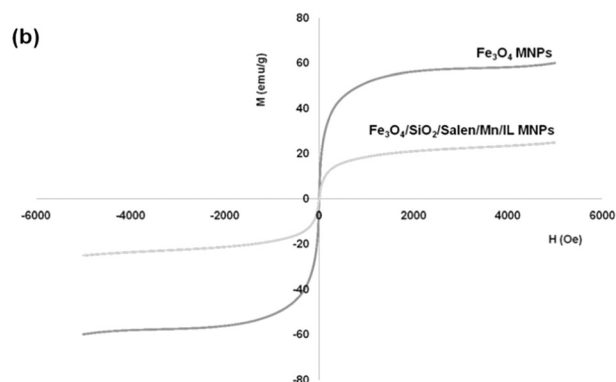
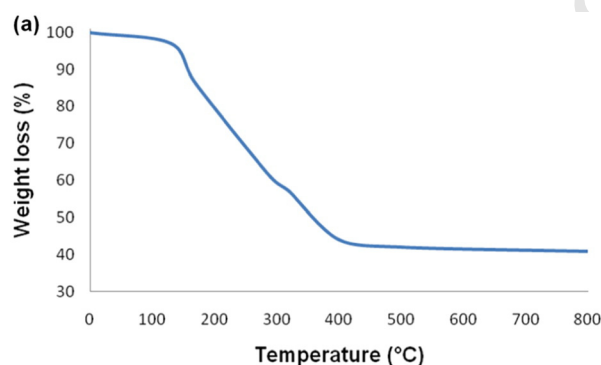


**Fig. 2.** (a) TGA diagram of  $\text{Fe}_3\text{O}_4/\text{SiO}_2/\text{Salen}/\text{Mn}/\text{IL}$  MNPs, and (b) Room-temperature magnetization curves of the  $\text{Fe}_3\text{O}_4$  and  $\text{Fe}_3\text{O}_4/\text{SiO}_2/\text{Salen}/\text{Mn}/\text{IL}$  MNPs.

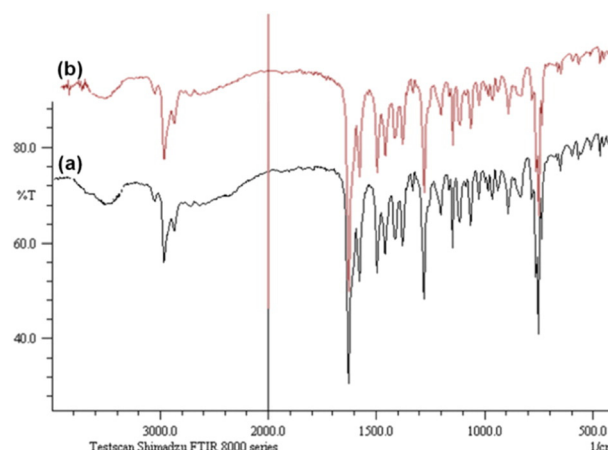


**Fig. 3.** FTIR spectra of (a)  $\text{Fe}_3\text{O}_4/\text{SiO}_2/\text{Salen}/\text{Mn}/\text{IL}$  MNPs, and (b) recovered  $\text{Fe}_3\text{O}_4/\text{SiO}_2/\text{Salen}/\text{Mn}/\text{IL}$  MNPs.

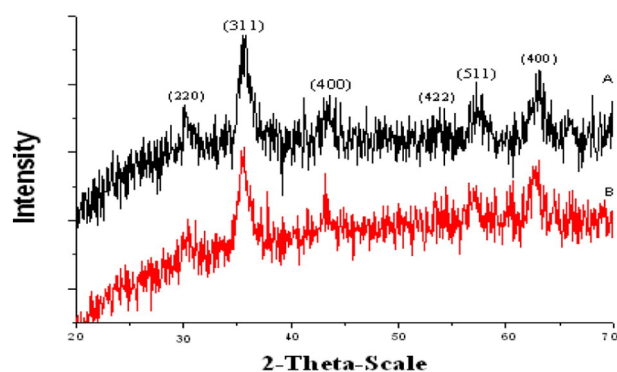


Fig. 4. XRD pattern of (A)  $\text{Fe}_3\text{O}_4$  MNPs and (B)  $\text{Fe}_3\text{O}_4/\text{SiO}_2/\text{Salen}/\text{Mn}/\text{IL}$  MNPs.

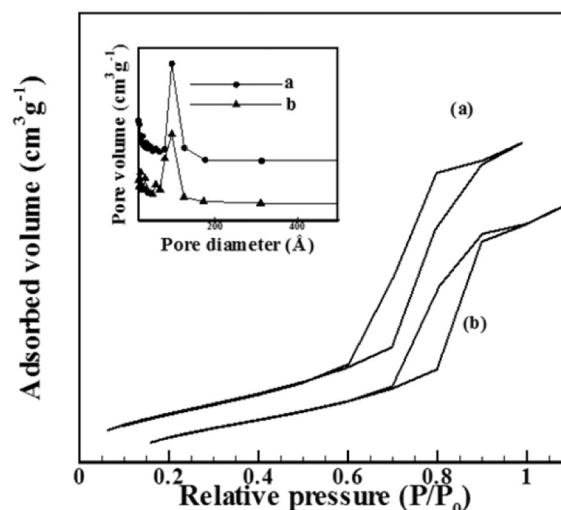


Fig. 6. Adsorption-desorption isotherms of (a)  $\text{Fe}_3\text{O}_4$  MNPs and (b)  $\text{Fe}_3\text{O}_4/\text{SiO}_2/\text{Salen}/\text{Mn}/\text{IL}$  MNPs.

8.2 Hz, 2H), 6.72 (s, 1H), 3.98 (d,  $J = 15.7$  Hz, 1H), 3.78 (d,  $J = 15.8$  Hz, 1H), and 2.18 (s, 3H) ppm.

### 3. Results and discussion

The  $\text{Fe}_3\text{O}_4/\text{SiO}_2$  core shell was synthesized by a simple method and then functionalized by the Schiff base complex of Mn (III), which had been obtained by the reaction between Mn (III) acetate and the Schiff base prepared from 1,2-benzenediamine and salicylaldehyde, according to Scheme 3. Then  $\text{Fe}_3\text{O}_4/\text{SiO}_2/\text{Salen}/\text{Mn}/\text{IL}$  MNPs was synthesized due to strong coordination between the metal center and the amino group of the IL. The synthesized  $\text{Fe}_3\text{O}_4/\text{SiO}_2/\text{Salen}/\text{Mn}/\text{IL}$  MNPs was then characterized by different methods such as XRD, TEM, VSM, FTIR and TGA.

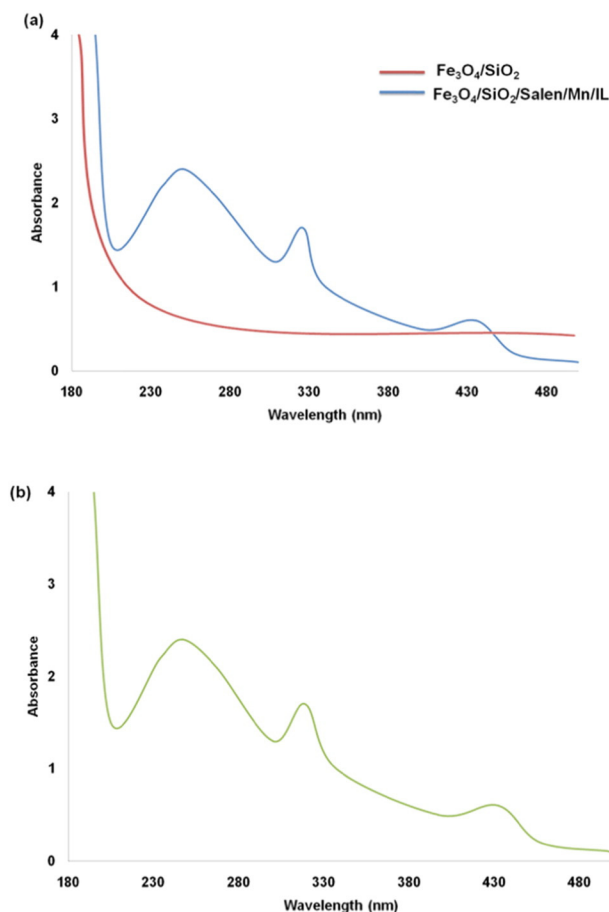


Fig. 5. UV-vis of (a)  $\text{Fe}_3\text{O}_4/\text{SiO}_2/\text{Salen}/\text{Mn}/\text{IL}$ ; (b)  $\text{Fe}_3\text{O}_4/\text{SiO}_2/\text{Salen}/\text{Mn}/\text{IL}$  MNPs after six reuses.

The particle size distribution of  $\text{Fe}_3\text{O}_4/\text{SiO}_2/\text{Salen}/\text{Mn}/\text{IL}$  MNPs was evaluated using transmission electron microscopy (TEM) and showed that the mean diameter of MNPs is 20–30 nm (Fig. 1).

The thermal behavior of  $\text{Fe}_3\text{O}_4/\text{SiO}_2/\text{Salen}/\text{Mn}/\text{IL}$  MNPs is shown in Fig. 2a. A significant decrease in the weight percentage of the  $\text{Fe}_3\text{O}_4/\text{SiO}_2/\text{Salen}/\text{Mn}/\text{IL}$  MNPs at about 130 °C is related to desorption of water molecules from the catalyst surface. This was evaluated to be 1–3% according to the TG analysis. A second, exothermic loss in weight of 11% appears at 230 °C and is followed by an additional large weight loss of 24% at 320 °C. This process extends up to ca. 400 °C. Above this temperature, the remaining organic material oxidizes up to 440 °C. The non-removable residue of ca. 12% belongs to the formation of manganese oxide and the sample remained dark. These results were in agreement with those obtained by ICP. The ICP analysis showed that 0.59 mmol of IL was anchored on 1.2 g of MNPs.

The magnetic properties of the nanoparticles were characterized using a vibrating sample magnetometer (VSM). The magnetization curves of the obtained nanocomposite registered at 300 K show nearly no residual magnetism is detected (Fig. 2b), which means that the nanocomposite exhibited the paramagnetic characteristics. Magnetic measurement shows that pure  $\text{Fe}_3\text{O}_4$ , and  $\text{Fe}_3\text{O}_4/\text{SiO}_2/\text{Salen}/\text{Mn}/\text{IL}$  MNPs have saturation magnetization values of 59.2, and 18.4 emu/g respectively. These nanocomposites with paramagnetic characteristics and high magnetization values can quickly respond to the external magnetic field and quickly redisperse once the external magnetic field is removed. The result reveals that the nanocomposite exhibit good magnetic responsible, which suggests a potential application for targeting and separation.

The successful synthesis of the  $\text{Fe}_3\text{O}_4/\text{SiO}_2/\text{Salen}/\text{Mn}/\text{IL}$  MNPs was confirmed by the FTIR spectra (Fig. 3a). In FTIR spectra of the  $\text{Fe}_3\text{O}_4/\text{SiO}_2$  MNPs, the absorption intensity of Fe–O group decreases with the addition of silica portion and a strong absorption intensity of the Si–O–Si group appears at 1090  $\text{cm}^{-1}$  owing to the silica coat. Peak appeared at 3120  $\text{cm}^{-1}$ , 2930  $\text{cm}^{-1}$ , 1620  $\text{cm}^{-1}$ , and 1510  $\text{cm}^{-1}$  are due to the stretching of the C–H aromatic group, the C–H aliphatic group, C=O group, and C=N group in the  $\text{Fe}_3\text{O}_4/\text{SiO}_2/\text{Salen}/\text{Mn}/\text{IL}$

Table 1  
BET result of  $\text{Fe}_3\text{O}_4$ , and  $\text{Fe}_3\text{O}_4/\text{SiO}_2/\text{Salen}/\text{Mn}/\text{IL}$  MNPs.<sup>a</sup>

Entry	Catalyst/cycle reusability	Specific surface area ( $\text{m}^2/\text{g}$ )	Pore volume ( $\text{cm}^3/\text{g}$ )	Average pore radius (nm)
1	$\text{Fe}_3\text{O}_4$	539	0.798	1.01
2	$\text{Fe}_3\text{O}_4/\text{SiO}_2/\text{Salen}/\text{Mn}/\text{IL}$	472	0.750	1.85

<sup>a</sup> Calculated by the BJH method.



**Table 2**

Optimization of the reaction conditions for the synthesis of 1,3-thiazolidin-4-one in terms of temperature, amount catalyst, time and product yield.

Entry	Catalyst	Solvent	Temp. (°C)	Time (min)	Amount catalyst (g)	Yield (%) <sup>a</sup>
1	Fe <sub>3</sub> O <sub>4</sub> /SiO <sub>2</sub> /Salen/Mn/IL	–	r.t.	50	0.001	94
2	Fe <sub>3</sub> O <sub>4</sub> /SiO <sub>2</sub> /Salen/Mn/IL	H <sub>2</sub> O	r.t.	50	0.001	23
3	Fe <sub>3</sub> O <sub>4</sub> /SiO <sub>2</sub> /Salen/Mn/IL	EtOH	r.t.	50	0.001	48
4	Fe <sub>3</sub> O <sub>4</sub> /SiO <sub>2</sub> /Salen/Mn/IL	THF	r.t.	50	0.001	37
5	Fe <sub>3</sub> O <sub>4</sub> /SiO <sub>2</sub> /Salen/Mn/IL	CH <sub>2</sub> Cl <sub>2</sub>	r.t.	50	0.001	24
6	Fe <sub>3</sub> O <sub>4</sub> /SiO <sub>2</sub> /Salen/Mn/IL	<i>n</i> -Hexane	r.t.	50	0.001	14
7	Fe <sub>3</sub> O <sub>4</sub> /SiO <sub>2</sub> /Salen/Mn/IL	–	80	50	0.001	94
8	Fe <sub>3</sub> O <sub>4</sub> /SiO <sub>2</sub> /Salen/Mn/IL	–	90	50	0.001	94
9	Fe <sub>3</sub> O <sub>4</sub> /SiO <sub>2</sub> /Salen/Mn/IL	–	100	50	0.001	94
10	Fe <sub>3</sub> O <sub>4</sub> /SiO <sub>2</sub> /Salen/Mn/IL	–	r.t.	40	0.001	94
11	Fe <sub>3</sub> O <sub>4</sub> /SiO <sub>2</sub> /Salen/Mn/IL	–	r.t.	30	0.001	94
12	Fe <sub>3</sub> O <sub>4</sub> /SiO <sub>2</sub> /Salen/Mn/IL	–	r.t.	20	0.001	73
13	Fe <sub>3</sub> O <sub>4</sub> /SiO <sub>2</sub> /Salen/Mn/IL	–	r.t.	30	0.0008	94
14	Fe <sub>3</sub> O <sub>4</sub> /SiO <sub>2</sub> /Salen/Mn/IL	–	r.t.	30	0.0006	75
15	–	–	r.t.	30	0.0008	–
16	Fe <sub>3</sub> O <sub>4</sub>	–	r.t.	30	0.0008	–
17	Fe <sub>3</sub> O <sub>4</sub> /SiO <sub>2</sub> /Salen	–	r.t.	30	0.0008	–
18	Fe <sub>3</sub> O <sub>4</sub> /SiO <sub>2</sub> /Salen/Mn	–	r.t.	30	0.0008	72

<sup>a</sup> Isolated yields.

MNPs. Furthermore, the IL-functionalized samples exhibited an additional feature at 3308 and 621 cm<sup>−1</sup> assigned to the stretching vibration of N–H groups and characteristic peaks of imidazole fragment, respectively. These observations suggest that the IL has been successfully bonded with the Salen Mn(III) complex.

The XRD pattern of Fe<sub>3</sub>O<sub>4</sub>/SiO<sub>2</sub>/Salen/Mn/IL MNPs by the corresponding reflections of (220), (311), (400), (422), (511) and (440) crystal planes as indicated in Fig. 4B. Comparing with XRD pattern of Fe<sub>3</sub>O<sub>4</sub> (Fig. 4A) and Fe<sub>3</sub>O<sub>4</sub>/SiO<sub>2</sub>/Salen/Mn/IL MNPs (Fig. 4B), immobilization manganese complex and IL on the surface of Fe<sub>3</sub>O<sub>4</sub> nanoparticles did not significantly affect the structure of nanoparticles.

The UV–vis spectra of neat complex and the supported ionic liquid catalysts are given in Fig. 5. The spectra of the supported ionic liquid catalysts showed features similar to those of the neat complex. The bands at 250 and 326 nm can be attributed to the charge transfer transition of Salen ligand. The band at 435 nm is due to ligand-to-metal charge transfer transition of Mn(III) Salen complex. On immobilization of Mn(III) Salen complex, all the characteristic bands appeared in its spectra. The UV–vis spectra confirmed the immobilization of Mn(III) Salen complex on the supports.

N<sub>2</sub> adsorption measurements, which have been a powerful tool for nano- or mesoporous material characterization, were performed to attain more insights into the modified Fe<sub>3</sub>O<sub>4</sub>. The samples displayed a type IV isotherm (as defined by IUPAC) with H<sub>1</sub> hysteresis and a sharp increase in pore volume adsorbed above P/P<sub>0</sub> 0.6–0.7 cm<sup>3</sup>/g, which is a characteristic of highly ordered mesoporous materials (Fig. 6). The textural properties of Fe<sub>3</sub>O<sub>4</sub> were substantially maintained over ionic liquid functionalization and subsequent complexation with Mn–Salen complex. A sharp decrease in surface area was observed for Fe<sub>3</sub>O<sub>4</sub> and Fe<sub>3</sub>O<sub>4</sub>/SiO<sub>2</sub>/Salen/Mn/IL MNPs from 539 to 472 m<sup>2</sup>/g, respectively, and the average pore volume decreased from 0.798 to 0.750 cm<sup>3</sup>/g

**Table 3**

Comparative of the catalytic activity of Fe<sub>3</sub>O<sub>4</sub>/SiO<sub>2</sub>/Salen/Mn/IL MNPs with Salen/Mn/IL.

Entry	Reaction time (min)	Yield (%) <sup>a</sup>	
		Fe <sub>3</sub> O <sub>4</sub> /SiO <sub>2</sub> /Salen/Mn/IL	Salen/Mn/IL
1	10	54	51
2	20	73	58
3	30	94	87
4	40	94	95
5	50	94	95

<sup>a</sup> Isolated yields.

**Table 4**

Synthesis of 1,3-thiazolidin-4-one derivatives catalyzed by Fe<sub>3</sub>O<sub>4</sub>/SiO<sub>2</sub>/Salen/Mn/IL MNPs.<sup>a</sup>

Entry	R <sub>1</sub>	R <sub>2</sub>	Product	Yield (%) <sup>b</sup>	Mp
1	Me	Me	4a	94	121–123 [38]
2	H	Me	4b	91	105–107 [38]
3	NO <sub>2</sub>	Me	4c	90	157–159
4	H	H	4d	93	129–131 [38]
5	Cl	H	4e	94	122–124 [38]
6	Me	H	4f	88	116–118 [38]
7	NO <sub>2</sub>	H	4g	92	105–107 [38]
8	H	Cl	4h	90	121–123 [38]
9	H	NO <sub>2</sub>	4i	92	160–162 [38]

<sup>a</sup> Reaction condition: aldehyde (1 mmol), amine (1 mmol), thioglycolic acid (1 mmol), and Fe<sub>3</sub>O<sub>4</sub>/SiO<sub>2</sub>/Salen/Mn/IL MNPs (0.0008 g) at room temperature under solvent-free conditions.

<sup>b</sup> Yield refers to isolated product.

(Table 1). The average pore diameters also decreased from 1.01 to 1.85 nm. This suggests that ionic liquids and the Mn–Salen complex may be well confined in the pores of the Fe<sub>3</sub>O<sub>4</sub>.

The catalytic potential of the Fe<sub>3</sub>O<sub>4</sub>/SiO<sub>2</sub>/Salen/Mn/IL MNPs was evaluated in condensation reactions. At first, the reaction of aldehyde, amine, and thioglycolic acid was chosen as a model reaction to optimize the reaction conditions such as amount of the catalyst, temperature, time, and solvent (Table 2). It was found that the best yield of the product was obtained at room temperature under solvent-free conditions in the presence of 0.0008 g of Fe<sub>3</sub>O<sub>4</sub>/SiO<sub>2</sub>/Salen/Mn/IL MNPs for 30 min (Table 2, entry 13). Three separated reactions were examined in the absence of any catalyst and in the presence of Fe<sub>3</sub>O<sub>4</sub> and Fe<sub>3</sub>O<sub>4</sub>/SiO<sub>2</sub>/Salen MNPs. The results of these studies showed that any amount of the desired product was not formed (Table 2, entries 15–17). A similar reaction in the presence of Fe<sub>3</sub>O<sub>4</sub>/SiO<sub>2</sub>/Salen/Mn MNPs as a non-supported catalyst gave the desired product in moderate yield (72%) due to the formation of by-products (Table 2, entry 18). This result indicated that the catalytic efficiency of IL was increased by immobilization onto Fe<sub>3</sub>O<sub>4</sub>/SiO<sub>2</sub>/Salen/Mn MNPs.

The catalytic activity of the Fe<sub>3</sub>O<sub>4</sub>/SiO<sub>2</sub>/Salen/Mn/IL MNPs was compared with the Salen/Mn/IL. For this purpose, the reactions were carried out separately at room temperature under solvent-free conditions with both the catalysts for the appropriate time (Table 3). The aliquots of the reaction mixture were collected periodically at an interval of 10 min. Table 3 shows the variation of the percentage preparation of 1,3-thiazolidin-4-one with time, when Fe<sub>3</sub>O<sub>4</sub>/SiO<sub>2</sub>/Salen/Mn/IL MNPs and Salen/Mn/IL were employed as catalysts. It is evident that, the catalytic activity of the Fe<sub>3</sub>O<sub>4</sub>/SiO<sub>2</sub>/Salen/Mn/IL MNPs is similar the Salen/Mn/IL. After 30 min Fe<sub>3</sub>O<sub>4</sub>/SiO<sub>2</sub>/Salen/Mn/IL MNPs showed 94% preparation of 1,3-thiazolidin-4-one as compared to 87% with Salen/Mn. After 40 min yield of the product in the presence of Fe<sub>3</sub>O<sub>4</sub>/SiO<sub>2</sub>/Salen/Mn/IL

**Table 5**

Comparison of the catalytic efficiency of Fe<sub>3</sub>O<sub>4</sub>/SiO<sub>2</sub>/Salen/Mn/IL MNPs with various catalysts.

Entry	Catalyst	Yield (%) <sup>a</sup>
1	Fe <sub>3</sub> O <sub>4</sub> /SiO <sub>2</sub> /Salen/Mn/IL MNP	94
2	H <sub>3</sub> PW <sub>12</sub> O <sub>40</sub>	69
3	NbCl <sub>5</sub>	–
4	PEG–SO <sub>3</sub> H	–
5	InCl <sub>3</sub>	62
6	Pd(PPh <sub>3</sub> ) <sub>4</sub>	30
7	Cerium(IV) ammonium nitrate	–
8	Nano-SiO <sub>2</sub>	78
9	Nano-RuO <sub>2</sub>	67
10	Nano-TiO <sub>2</sub>	40
11	Nano-Pd	53
12	Nano-FeNi <sub>3</sub>	42

<sup>a</sup> Reaction conditions aldehyde (1 mmol), amine (1 mmol), and thioglycolic acid (1 mmol) at room temperature under solvent-free conditions for 30 min.

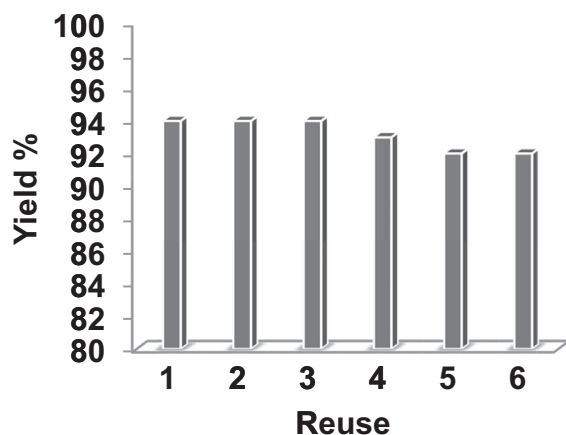


Fig. 7. Reuses performance of the catalysts.

#### 4. Conclusion

In conclusion, we have developed a heterogeneous catalyst based on the concept of supported ionic liquid phase catalysis. The amounts of both ionic liquids as well as the transition metal species involved in the preparation of catalysts were low and the preparation procedure was easy, thus displaying very good performance from an economic point of view. The catalyst was well characterized by different physicochemical techniques to confirm its structural integrity. The synthesized  $\text{Fe}_3\text{O}_4/\text{SiO}_2/\text{Salen}/\text{Mn}/\text{IL}$  MNP was used as a magnetically recyclable heterogeneous catalyst for the efficient one-pot synthesis of 1,3-thiazolidin-4-ones from the reaction of aldehyde, amine, and thioglycolic acid with high product yields. This catalyst offers notable advantages such as heterogeneous nature, easy separation by external magnetic field, good to excellent product yields, easy preparation, short reaction times, and simplicity of handling. In addition, the catalyst used is easily recovered by using an external permanent magnet and reused without any noticeable loss of activity after at 6 times.

#### References

- Y.X. Li, X. Zhai, W.K. Liao, *Chin. Chem. Lett.* 23 (2012) 415–418.
- D. Bhambhani, V.K. Salvi, J.L. Jat, S. Ojha, G.L. Talesara, *J. Sulfur Chem.* 28 (2007) 155–163.
- X. Zhang, X. Li, D. Li, *Bioorg. Med. Chem. Lett.* 19 (2009) 6280–6283.
- A. Mobinikhaledi, N. Foroughifar, M. Kalhor, *J. Heterocycl. Chem.* 47 (2010) 77–80.
- X. Jin, C.J. Zheng, M.X. Song, *Eur. Med. Chem.* 56 (2012) 203–209.
- X.J. Sun, W.L. Dong, W.G. Zhao, Z.M. Li, *Chin. J. Org. Chem.* 27 (2007) 1374–1380.
- B. Chandrasekhar, *J. Sulfur Chem.* 29 (2008) 187–240.
- D. Gautam, P. Gautam, R.P. Chaudhary, *Chin. Chem. Lett.* 23 (2012) 1221–1224.
- S.G. Patil, R.R. Bagul, M.S. Swami, *Chin. Chem. Lett.* 22 (2011) 883–886.
- V. Gududuru, V. Nguyen, J.T. Dalton, D.D. Miller, *Synlett* (2004) 2357–2358.
- U.R. Pratap, D.V. Jawale, M.R. Bhosle, R.A. Mane, *Tetrahedron Lett.* 52 (2011) 1689–1691.
- P.J. Wasserscheid, W. Keim, *Angew. Chem. Int. Ed.* 39 (2000) 3772–3789.
- T. Welton, *Chem. Rev.* 99 (1999) 2071–2084.
- T. Selvam, A. Machoke, W. Schwieger, *Appl. Catal. A Gen.* 445–446 (2012) 92–101.
- Y.H. Kim, S. Shin, H.J. Yoon, J.W. Kim, J.K. Cho, Y.S. Lee, *Catal. Commun.* 40 (2013) 18–22.
- J. Miao, H. Wan, Y. Shao, G. Guan, B. Xu, *J. Mol. Catal. A: Chem.* 348 (2011) 77–82.
- K. Dhara, K. Sarkar, D. Srimani, S.K. Saha, P. Chattopadhyay, A. Bhaumik, *Dalton Trans.* 39 (2010) 6395–6402.
- S. Paul, J.H. Clark, *Green Chem.* 5 (2003) 635–638.
- H. Oju, S.M. Sarkar, D.-H. Lee, M.J. Jin, *Green Chem.* 10 (2008) 37–40.
- G.S. Mishra, A. Kumar, *Catal. Sci. Technol.* 1 (2011) 1224–1231.
- N.T.S. Phan, D.H. Brown, P. Styring, *Tetrahedron Lett.* 45 (2004) 7915–7919.
- Y. He, C. Cai, *Catal. Commun.* 12 (2011) 678–683.
- Y.X. Liu, Z.W. Ma, J. Jia, C.C. Wang, M.L. Huang, J.C. Tao, *Appl. Organomet. Chem.* 24 (2011) 646–649.
- Z. Wang, P. Xiao, N. Shen, B. He, *Colloids Surf. A Physicochem. Eng. Asp.* 276 (2006) 116–121.
- A. Schätz, M. Hager, O. Reiser, *Adv. Funct. Mater.* 19 (2009) 2109–2115.
- F. Zhang, J. Jin, X. Zhong, S. Li, J. Niu, R. Li, J. Ma, *Green Chem.* 13 (2011) 1238–1242.
- J. Mondal, T. Sen, A. Bhaumik, *Dalton Trans.* 41 (2012) 6173–6181.
- C.W. Lim, I.S. Lee, *Nano Today* 5 (2010) 412–434.
- V. Polshettiwar, R.S. Varma, *Green Chem.* 12 (2010) 743–754.
- V. Polshettiwar, R. Luque, A. Fihri, H. Zhu, M. Bouhrara, J.M. Basset, *Chem. Rev.* 111 (2011) 3036–3075.
- J. Lu, X.T. Li, E.Q. Ma, L.P. Mo, Z.H. Zhang, *ChemCatChem* 6 (2014) 2854–2859.
- J. Deng, L.P. Mo, F.Y. Zhao, L.L. Hou, L. Yang, Z.H. Zhang, *Green Chem.* 13 (2011) 2576–2584.
- Y.H. Liu, J. Deng, J.W. Gao, Z.H. Zhang, *Adv. Synth. Catal.* 354 (2012) 441–447.
- P.H. Li, B.L. Li, Z.M. An, L.P. Mo, Z.S. Cui, Z.H. Zhang, *Adv. Synth. Catal.* 355 (2013) 2952–2959.
- F.P. Ma, P.H. Li, B.L. Li, L.P. Mo, N. Liu, H.J. Kang, Y.N. Liu, Z.H. Zhang, *Appl. Catal. A Gen.* 457 (2013) 34–41.
- R. Tan, D. Yin, N. Yu, Y. Jin, H. Zhao, D. Yin, *J. Catal.* 255 (2008) 287–295.
- S.M. Sadeghzadeh, F. Daneshfar, M. Malekzadeh, *Chin. J. Chem.* 32 (2014) 349–355.
- A. Bolognese, G. Correale, M. Manfra, *Org. Biomol. Chem.* 2 (2004) 2809–2813.

MNPs is fixed in 94% but  $\text{Salen}/\text{Mn}/\text{IL}$  MNPs showed 95% preparation of 1,3-thiazolidin-4-one. The nano-sized particles increase the exposed surface area of the active component of the catalyst, thereby enhancing the contact between reactants and catalyst dramatically and mimicking the homogeneous catalysts. Also, the activity and selectivity of nano-catalyst can be manipulated by tailoring chemical and physical properties like size, shape, composition and morphology.

After optimization of the reaction conditions, to delineate this approach, particularly with regard to library construction, this methodology was evaluated by using different amines, variety of different substituted aldehyde and of thioglycolic acid in the presence of 1,3-thiazolidin-4-ones MNPs under similar conditions. As can be seen from Table 4, electronic effects and the nature of substituents on the amines and aldehyde did not show strongly obvious effects in terms of yields under the reaction conditions. The three-component cyclocondensation reaction proceeded smoothly.

In order to show the unique catalytic behavior of  $\text{Fe}_3\text{O}_4/\text{SiO}_2/\text{Salen}/\text{Mn}/\text{IL}$  MNPs in these reactions, we have performed one-pot reaction of aldehyde, amine, and thioglycolic acid in the presence of a catalytic amount of  $\text{H}_3\text{PW}_{12}\text{O}_{40}$ ,  $\text{NbCl}_5$ ,  $\text{PEG-SO}_3\text{H}$ ,  $\text{InCl}_3$ ,  $\text{Pd}(\text{PPh}_3)_4$ , cerium(IV) ammonium nitrate, nano- $\text{SiO}_2$ , nano- $\text{RuO}_2$ , nano- $\text{TiO}_2$ , nano- $\text{Pd}$ , and nano- $\text{FeNi}_3$  (Table 5). As it is evident from Table 5,  $\text{Fe}_3\text{O}_4/\text{SiO}_2/\text{Salen}/\text{Mn}/\text{IL}$  MNPs is the most effective catalyst for this purpose, leading to the formation of 1,3-thiazolidin-4-one in a good yield.

It is important to note that the magnetic property of  $\text{Fe}_3\text{O}_4/\text{SiO}_2/\text{Salen}/\text{Mn}/\text{IL}$  MNPs facilitates its efficient recovery from the reaction mixture during work-up procedure. The activity of the recycled catalyst was also examined under the optimized conditions. After the completion of reaction, the catalyst was separated by an external magnet, washed with methanol and dried at the pump. The recovered catalyst was reused for six consecutive cycles without any significant loss in catalytic activity (Fig. 7). In order to know whether the reaction takes place at the surface of  $\text{Fe}_3\text{O}_4/\text{SiO}_2/\text{Salen}/\text{Mn}/\text{IL}$  MNPs as a truly heterogeneous catalyst or any IL species as a homogeneous catalyst, ICP analysis of the remaining mixture after catalyst and product separation was investigated upon reaction completion. The amount of IL leaching after the six repeated recycling was 3.8%. These observations indicated that the catalyst was stable and could tolerate the present reaction conditions.

The recyclability test was stopped after six runs. Comparison of TEM images (Fig. 1b), FT-IR spectra (Fig. 3b), and UV/vis spectra (Fig. 5b) of used catalyst with those of the fresh catalyst (Figs. 1a, 3a, and 5a) showed that the morphology and structure of  $\text{Fe}_3\text{O}_4/\text{SiO}_2/\text{Salen}/\text{Mn}/\text{IL}$  MNPs remained intact after six recoveries.